Physics of Fluids

RESEARCH ARTICLE | JUNE 03 2024

Micropolar effects on the effective shear viscosity of nanofluids FREE

R. Bondarenko; Yu. Bukichev; A. Dzhaga; G. Dzhardimalieva; Y. Solyaev

Check for updates

Physics of Fluids 36, 062004 (2024)
https://doi.org/10.1063/5.0208850

View Online

Export Citation

AIP Publishing

Physics of Fluids ARTICLE pubs.aip.org/aip/pof

Micropolar effects on the effective shear viscosity of nanofluids

Cite as: Phys. Fluids **36**, 062004 (2024); doi: 10.1063/5.0208850
Submitted: 17 March 2024 · Accepted: 13 May 2024 ·
Published Online: 3 June 2024

R. Bondarenko,[1] Yu. Bukichev,[2,3] A. Dzhaga,[1] G. Dzhardimalieva,[2,3] and Y. Solyaev[1,2,a)]

AFFILIATIONS

[1]Institute of Applied Mechanics of Russian Academy of Sciences, Moscow, Russia
[2]Moscow Aviation Institute, Moscow, Russia
[3]Federal Research Center of Problems of Chemical Physics and Medicinal Chemistry RAS, Chernogolovka, Russia

[a)]**Author to whom correspondence should be addressed:** yos@iam.ras.ru

ABSTRACT

The modified size-dependent Einstein's and Brinkman's solutions are established for the effective shear viscosity of rigid particle suspensions taking into account the micropolar effects in the base fluid. Solutions are obtained based on the homogenization approach and allow us to take into account the influence of the particle size. Two non-classical parameters arise in the considered micropolar solutions: the length scale parameter and the coupling (micropolarity) number of the base fluid. The solutions developed are validated using tests performed with polydimethylsiloxane based TiO_2 nanofluids as well as other published data on the size-dependent shear viscosity of different nanofluids. Good agreement between the predictions and the experimental data is established across a wide range of volume fractions and size of nanoparticles. The possibility for unique identification (at given temperature) of the micropolar parameters of the base fluids is shown. Temperature-dependent values of non-classical rotational and spin viscosities of polydimethylsiloxane, ethylene glycol, and water are evaluated.

I. INTRODUCTION

Nanofludis are engineered liquid suspensions containing nano-sized solid particles that can be used in a wide class of applications related to heat transfer, hydraulics, lubricants, medicine, energy harvesting, etc.[1] The physical properties of nanofluids are strongly affected by their volume fraction and size, as well as their shape, Brownian motion, and interactions (agglomeration), temperature and pH value of the base fluid.[2,3] Different theoretical models have been suggested for evaluating the effective properties of nanofluids within the continuum mechanics, molecular dynamics, and semi-empirical methods (for review, see Refs. 4–7). The main peculiarity of these models is the capturing of size effects, i.e., change in their effective properties with change in the particles size, that have been widely investigated for effective thermal conductivity and shear viscosity of nanofluids.[2,8]

One of the main factors playing a predominant role in the nature of size effects in nanofluids is the adsorption of base fluid molecules on the surface of particles.[3,9–11] The adsorbed layers have modified physical properties in comparison to the base fluid. Since the surface of nano-sized particles becomes extremely large, the influence of the adsorbed layers on the overall properties of nanofluids becomes significant. In theoretical models, the structure of adsorbed layers can be directly studied within the molecular dynamics method,[3,10] or it can be introduced as the "third phase" between the particles and the base fluids in continuum models.[9,12,13]

In the present study, we show that an alternative approach for the analysis of the size-dependent shear viscosity of nanofluids can be used considering micropolar effects in the base fluid. The micropolar theory of fluids has been developed by Dahler[14] and Eringen,[15] and it is also known as the theory of polar fluids[16] or the extended Navier–Stokes theory.[17] The micropolar theory considers an independent rotational velocity of a fluid particle in addition to the standard translational velocity. The formulation of the micropolar theory and the basic theoretical results in this field can be found elsewhere.[15–19] Over the last decades, it has been shown that the micropolar theory can be effectively used for the refined analysis of fluid flows at the nano-scale since the independent field of rotation can be related to the self-spinning of fluid molecules.[20–23] The extended definition of boundary conditions with constrained rotations in addition to standard no-slip conditions allows one to evaluate the behavior of liquids at scales that are comparable to the size of their molecules.[22] Such generalized adhesive conditions can be used to simulate the presence of adsorbed layers of fluid molecules on the solid surfaces.[15]

The constitutive equations of micropolar theory contain additional material constants that are the so-called rotational and spin viscosities.[16,24] The non-dimensional analysis is usually performed in terms of related parameters: the coupling (micropolarity) number and the length scale parameter.[16] Experimental methods for the determination of these parameters based on the measurements of the apparent flow rate in small-scale channels have been proposed.[25,26] Validation of the micropolar theory of fluids via the molecular dynamics simulations for nano-scale flows has also been shown.[20,24]

Applying micropolar theory to simulate the effective shear viscosity of suspensions relies on solving the problem of the creeping shear flow past a sphere.[27,28] A classical solution was developed by Einstein, who obtained his famous formula for the effective viscosity of dilute suspensions of rigid particles.[29] A generalization of Einstein's formula for concentrated suspensions has been provided by Brinkman via differential approach.[30] Other variants of generalized Einstein's solution for concentrated suspensions were developed later.[4] Nevertheless, these solutions within classical fluid mechanics are self-similar, i.e., they do not contain the length scale parameters and do not depend on the sphere size. In contrast, the corresponding solution for flow past a sphere within the micropolar theory does contain such parameters and allows consideration of the size effects.[27,28]

The closed-form solutions of micropolar theory for the effective viscosity of suspensions containing spherical particles have been previously developed by Erdogan,[31] Avudainayagam,[32] and Niefer and Kaloni.[33] However, in these works the authors used approximate ansatz for the velocity field[31] (this Erdogan's solution can be used only for relatively small values of coupling number) or approximate assessments on the amount of dissipated energy[32,33] around the particles embedded in the micropolar fluid. Application of a closed-form solution for the Poiseuille flow in a pipe for an assessment of apparent viscosity of suspensions has been proposed in Ref. 34.

In the present study, we derive a new variant of a closed-form solution for the effective shear viscosity of rigid particle suspensions in micropolar fluids. We obtain this solution in a more simple (in comparison to Refs. 31–33) though also rigorous way: by using the analogy between the theory of creeping incompressible flow of micropolar fluids and the corresponding micropolar theory for incompressible solids. This analogy has been discussed, e.g., in Ref. 35. From the micropolar theory of solids, we use the known solution for the homogenization problem for the composite with spherical inclusion at dilute concentrations.[36,37] Following the mentioned mathematical analogy between the theories, we convert the solution for micropolar solids to the generalized Einstein's formula for the case of micropolar fluids. Such a standard approach is well known in classical micromechanics, where the Einstein formula can be obtained based on the dilute solution for the effective shear modulus of composites with spherical inclusions.[38] In our recent work,[39] a similar approach has been used to obtain the size-dependent solution for the shear viscosity of nanofluids within the theory of high-grade hydrodynamics.[40]

In the present study, we derive the generalized variants of size-dependent solutions within the micropolar theory and provide its experimental validation. In our tests, we consider the widely used silicone oil (polydimethylsiloxane) with TiO_2 nanoparticles. Nanofluid samples at various volume fractions and particle sizes are tested at different temperatures to provide validation of the developed solutions. Similar known experimental data for the other types of nanofluids[41–43] are also processed by using derived solutions. Good agreement between theoretical and experimental results is obtained, and the unique values of the micropolar model parameters are identified. This makes the derived solutions preferable to our previous size-dependent models,[39] where we had to adjust the length scale parameters to describe size effects across a broader range of particle diameters. In comparison to the known semi-empirical size-dependent solutions,[4] the presented model has rigorous theoretical foundation and can also be used in inverse identification problems for the case of non-classical rotational and spin viscosities of base fluids. The corresponding examples of identification are given in this paper.

II. SIZE-DEPENDENT SOLUTIONS FOR THE EFFECTIVE VISCOSITY

In this section, we give a brief derivation of the size-dependent solutions for the effective shear viscosity of nanofluids within the micropolar theory. We follow an approach that is traditionally used in micromechanics and based on the analogy between the steady-state formulation of micropolar theory of fluids (for creeping flow) and micropolar elasticity. Moreover, we discuss the meaning of non-classical parameters that arise in the developed solutions and suppose a method for its identification.

A. Known results from micromechanics

We start with the known closed-form solution for the effective shear modulus of solid composite materials with spherical inclusions at dilute concentration. This solution is given by[44]

$$\mu^* = \mu + \frac{f\mu}{2S_{1212} + \dfrac{\mu}{\mu_i - \mu}}, \tag{1}$$

where μ and μ_i are the shear moduli of isotropic matrix and isotropic inclusions, respectively, μ^* is the effective shear modulus of the composite material, f is the volume fraction of inclusions, and S_{1212} is the component of the Eshelby tensor that should be found from the solution for the corresponding Eshelby problem with spherical inclusion embedded in infinite matrix.[44]

The representation for the Eshelby tensor depends on the theory under consideration, though in any kind of solution it contains only the material properties of the matrix and data on the shape and the size of the inclusion (the last one within the generalized continuum theories). In classical elasticity, the value of S_{1212} depends only on the Poisson ratio of the matrix phase ν as follows:[45]

$$S_{1212} = \frac{4-5\nu}{15(1-\nu)}. \tag{2}$$

Substituting (2) into (1) and evaluating the limit value for incompressible matrix $(\nu \to 1/2,\ S_{1212} \to 1/5)$ and rigid inclusions $(\mu_i \to \infty)$, one can obtain the classical Einstein's formula for composites with incompressible matrix and rigid inclusions:

$$\mu^* = \mu\left(1 + \frac{5}{2}f\right). \tag{3}$$

Taking into account the well-known mathematical analogy between the formulation of elasticity theory and the steady-state problem of fluid mechanics (for the creeping flow), we can consider this result (3) as the solution for the effective shear viscosity (μ^*) of a dilute suspension comprised of an incompressible base fluid with intrinsic shear viscosity μ, along with rigid particles at a volume fraction f.

Within the non-classical generalized continuum theories of solids, representation for the effective shear modulus remains the same as presented in Eq. (1), when one considers direct homogenization methods.[46,47] However, the value of the component of the Eshelby tensor S_{1212} should be treated as the average over the inclusion volume. This fact arises from the position-dependent solutions for Eshelby tensor within the generalized continuum theories, such that the strain gradient elasticity,[46] the surface elasticity[48] and the micropolar elasticity.[37,49] Precise capturing of the effects related to the nonuniform strain and stress states inside the inclusions (even for the homogeneous boundary conditions at the far field) can be performed only using the energy-based homogenization approaches within the generalized continuum theories.[50,51] Nevertheless, the direct homogenization methods and the presented relation (1) allow one to obtain simplified closed-form solutions that provide rather accurate assessments of the effective size-dependent properties of composites with volume fractions of inclusions that are not very large.[50]

Thus, let us consider the known solution of micropolar elasticity for the Eshelby tensor in the case of spherical inclusion. The component of the Eshelby tensor S_{1212} averaged over the volume of spherical inclusion of diameter d is given by[37]

$$S_{1212} = \frac{4-5\nu}{15(1-\nu)} + \frac{3}{5}\frac{N^2}{\bar{d}^3}\left(4 - \bar{d}^2 - (2-\bar{d})^2\ \mathrm{e}^{-\bar{d}}\right), \qquad (4)$$

where we do not introduce a new definition for the averaged quantity to simplify our presentation; N is the so-called non-dimensional coupling (micropolarity) number of the matrix material and $\bar{d} = Nd/\ell$ is the normalized diameter of sphere evaluated via the length scale parameter ℓ that is also the non-classical property of the matrix material.

Relation (4) presented here is expressed using slightly different notations compared to those utilized in the original paper.[37] The proposed notations are more useful for the following analysis and are also common in applied problems of the micropolar theory.[16,19] The relation between representation (4) and the one in Ref. 37 is given in Appendix B.

From thermodynamic considerations,[16] it is known that the coupling number can take values in the range $0 \leq N < 1$, while the length scale parameter should take real positive values, $\ell \geq 0$. It is easy to see that relation (4) will be reduced to the classic definition (2) in the case of zero coupling number, $N = 0$. This result corresponds to the case when the internal rotational motions of the material's particles have no effect on their overall response, i.e., the micro- and macro-scale deformations become uncoupled. The classical solution will also be obtained from (4) when we consider an infinitely small length scale parameter $\ell \to 0$ (or equivalently, $\bar{d} \to \infty$). This case corresponds to media with relatively large inclusions or with very fine internal microstructure that becomes negligible at the macroscale.

B. Solutions for incompressible micropolar media with rigid spherical inclusions

In the interest of the present study, let us consider the case of an incompressible matrix ($\nu \to 1/2$) and obtain the following result from (4):

$$S_{1212} = \frac{1}{5}F(N,\bar{d}), \quad F(N,\bar{d}) = 1 + 3\frac{N^2}{\bar{d}^{-3}}\left(4 - \bar{d}^2 - (2-\bar{d})^2\ \mathrm{e}^{-\bar{d}}\right), \qquad (5)$$

where we denote by $F(N,\bar{d})$ the non-classical size-dependent group of parameters.

Substituting (5) into (1) and assuming rigid behavior of inclusions ($\mu_i \to \infty$), we derive Einstein's formula generalized for the micropolar theory:

$$\mu^* = \mu\left(1 + \frac{5}{2F(N,\bar{d})}f\right). \qquad (6)$$

Based on the analogy between formulation of steady-state theories of micropolar fluids (for creeping flow) and micropolar solids, we can use solution (6) for assessing the effective shear viscosity of suspensions consisting of the incompressible base fluid and the rigid particles. This analogy for micropolar theories has been discussed by Cowin[16] and is also emphasized in Appendix A. Similar to classical theories, the effective shear modulus μ^* in (6) should be treated as the effective shear viscosity and μ should be the shear viscosity of the base fluid, while f is the volume fraction of spherical particles of diameter d. The micropolar parameters N and ℓ that arise in the definition of $F(N,\bar{d})$ become the intrinsic properties of the base fluid.

Then, the solution for the effective viscosity of concentrated suspensions in micropolar theory can be obtained based on relation (6) and a differential method.[44] Thus, we can evaluate the increase in effective viscosity $d\mu^*$ due to addition of a small amount of particles df as follows:

$$\mu + d\mu^* = \mu^*(df'), \qquad (7)$$

where $df' = df/(1-f)$ is the actual volume fraction of the added inclusions that takes into account the corresponding decrease in base fluid volume. This value (df') should be used in the definition of μ^* (6) instead of f and the result should be used in (7) to obtain the following differential relation:

$$\frac{d\mu^*}{df} = \frac{5\mu}{2(1-f)F(N,\bar{d})}. \qquad (8)$$

Solution of Eq. (8) together with the initial condition $\mu^*|_{f=0} = \mu$ provides us the final result for the Brinkman formula within the micropolar theory:

$$\mu^* = \frac{\mu}{(1-f)^{\frac{5}{2F(N,\bar{d})}}}. \qquad (9)$$

The classical solutions, i.e., the standard Einstein's formula (3) and classical Brinkman's formula,[30] can be recovered from (6) and (9) in the case of absence of coupling [$N = 0$, $\Phi(0,\bar{d}) = 1$] or in the case of relatively large particles [$\bar{d} \to \infty$, $\Phi(N,\infty) = 1$], as mentioned above. Our previous solutions obtained within high-grade theories[39] can also be derived from (6) and (9) assuming unit value for the coupling number, $N = 1$, corresponding to the well-known relation between the micropolar and the couple stress theory.[15] In solid mechanics, the last one is the particular variant of strain gradient elasticity and its solution for incompressible composites coincides with the general theory.[39]

To the best of the authors' knowledge, the presented solutions (6) and (9) have not been derived previously. The effective viscosity of dilute suspensions was evaluated in a form similar to (6) in Refs. 31–33. However, in these works the authors used an approximate ansatz for the velocity field[31] or approximate assessment of the amount of dissipated energy.[32,33] The solution presented here is also approximate, akin to the classical Einstein's formula (3), where it is expressed up to the linear term in concentration f. The use of differential method (9) allows us to extend its applications to higher concentrations. We also mention Ref. 52, where the authors suggested a correction to the standard Brinkman's solution in the form $\mu^* = \mu(1-f)^{-5\varepsilon/2}$, where $\varepsilon > 0$ is some coefficient, which is responsible for the influence of particle interactions (e.g., magnetic interactions[52]). As follows from the presented result (9), a similar correction also arises in Brinkman's solution due to certain intrinsic properties of the liquid.

C. Physical meaning of micropolar parameters and its experimental identification

The physical meaning of the non-classical micropolar parameters, N and ℓ, was discussed, e.g., in Refs. 16, 21, and 53. Both of these parameters naturally arise in the non-dimensional formulation of the governing equation of the micropolar theory (see Appendix A). The coupling (or micropolarity) number, N, formally defines the coupling of the conservation laws for the linear and angular momentum in micropolar media. This parameter can also be treated as a ratio of viscous forces of relative rotation to the standard Newtonian viscous forces.[16] The length scale parameter, ℓ, can be related to some characteristic size of the fluid inner microstructure, e.g., the size of molecules or the length of polymer chains.[18,20] The value of ℓ also defines the length of boundary layers that arise in micropolar solutions with additional restriction on rotations at the boundaries (no-spin condition).[15,16,22] From this point of view, the value of ℓ characterizes the length of adhesive interactions and the thickness of adsorbed molecular layers that arise at the solid/liquid boundary. Note that the initial solution for the Eshelby tensor (4) has been developed assuming continuity of the rotations at the boundary of inclusion and the surrounding material.[36,37] Thus, under the condition of rigid inclusion we obtain the solution that corresponds to the no-spin condition at the boundary of the particle.

Definitions for N and ℓ can be given in terms of standard and non-classical viscosity parameters of the fluid (see Appendix A and also Refs. 16, 19, and 22),

$$N = \sqrt{\frac{\kappa}{\mu+\kappa}}, \qquad \ell = \sqrt{\frac{\gamma}{4\mu}}, \tag{10}$$

where μ (Pa s) is the standard shear viscosity, while κ (Pa s) and γ (Pa s m^2) are the so-called rotational and spin viscosities,[24] i.e., the non-classical micropolar properties of the medium. In the present case of suspensions, these are the properties of the base fluid.

In the following, we will provide an assessment of the values of N and ℓ by using the experimental data on the dependence of the effective shear viscosity of suspensions μ^* on the mean size of filler particles. Illustrations for the size effects that can be captured within the derived solutions (6) and (9) are presented in Figs. 1 and 2. In Fig. 1, we show the predicted dependence of the normalized effective viscosity μ^*/μ on the volume fraction. Different curves in this figure correspond to different values of the coupling number, N, and relative size of inclusions, d/ℓ. It can be seen that the classical Einstein's and Brinkman's solutions ($N = 0$, black lines in Fig. 1) always predict lower viscosity than the micropolar solutions. The difference between the micropolar and classical solutions become even more pronounced at higher coupling and for smaller particles (green and yellow curves in Fig. 1). In this figure, it can be also seen that the range of volume fractions where the generalized Einstein's (dotted lines) and Brinkman's (solid lines) solutions give close predictions become narrower in comparison to classical theory. For the strong micropolar effects, close results are obtained for volume fractions not higher than $f = 2\%$–3%. Therefore, in the following, we will use the solution for concentrated suspension (9) for the processing of experimental data, where we will consider the volume fractions of nanoparticles up to 5%.

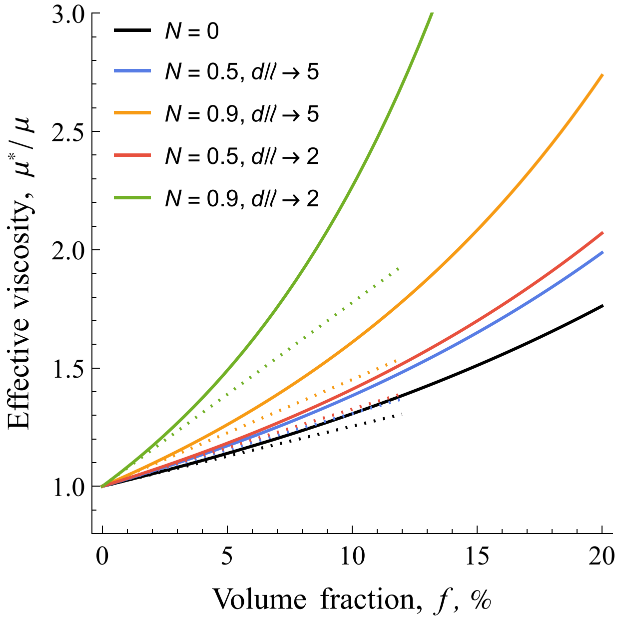

FIG. 1. Dependence of the effective shear viscosity of suspensions on the volume fraction of particles predicted by generalized Einstein's solution (6) (dotted lines) and Brinkman's solutions (9) (solid lines). Classical solutions are presented in black color.

In Fig. 2, we show the dependence of effective viscosity on the diameter of particles for different coupling numbers and length scale parameters of the base fluid. This dependence is incorporated into the developed solutions via the group of parameters denoted by $F(N, \bar{d})$ (5). For these plots, we used the absolute values of diameter and length scale parameter (in nanometers) to make more visual the type of size effects that can be described within the micropolar theory. We use typical ranges of these parameters for nanofluids. It can be seen that the micropolar theory can be used to describe the so-called positive size effects, i.e., the rise of nanofluid viscosity with decrease in the particle size. Such effects are rather common in nanofluids, though negative size effects and non-monotonic dependences are also known.[2] Thus, considering the micropolar theory without additional assumptions (e.g., on the possible agglomeration of particles), we should restrict our attention to experiments, where the positive size effects were observed.

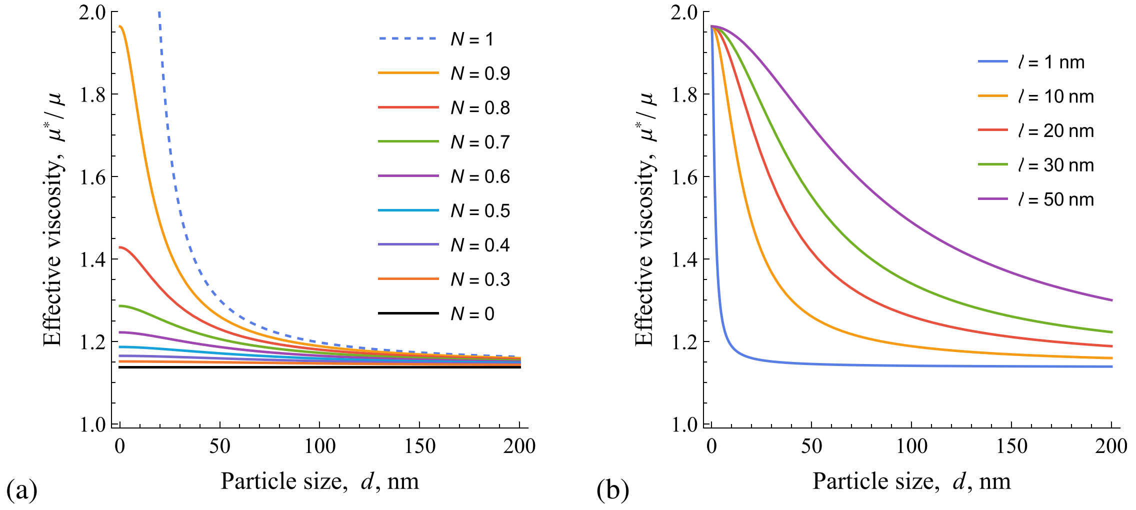

FIG. 2. Dependence of the effective shear viscosity of suspensions on particle size (d) at constant volume fraction $f = 5\%$ predicted by the generalized Brinkman's solution (9). (a) Results for various coupling numbers and fixed length scale parameter $\ell = 10$ nm and (b) results for various length scale parameters and fixed coupling number $N = 0.9$.

In Fig. 2(a), one can see that the value of the coupling number, N, controls the maximum possible rise of the suspension viscosity. For small values of N, the change in viscosity can be negligible, and it may have almost constant value as in classical solutions [$N = 0$, black line in Fig. 2(a)]. For the case $N = 1$, effective viscosity shows infinite rise for the smallest particles, i.e., $d \rightarrow 0$. This case ($N = 1$) corresponds to the high-grade theory that was considered in our previous work.[39] This solution becomes less flexible for describing size effects in nanofluids since it always predicts very rapid increase in viscosity for the smallest particles.

In Fig. 2(b), it is shown that the value of the length scale parameter ℓ influences the "rate" of size effect. For small values of ℓ, the increase in viscosity arises only for very small particles of the same order of ℓ, and it rapidly tends to the classical value with increase in particles size [blue line in Fig. 2(b)]. Conversely, for large values of ℓ, the size effect becomes very gradual and extends over a wide range of particle diameters [purple line in Fig. 2(b)].

To identify the non-classical parameters N and ℓ, we propose to fit the micropolar solutions (6) and (9) to the experimental data on the dependence of the effective shear viscosity of nanofluids on the average size of particles. Since two non-classical parameters persist in these solutions, we need at least two different experimental points. However, we cannot use the data for the viscosity of suspensions with different volume fraction of particles of the same size, since the identification of micropolar parameters will be non-unique in this case. This is illustrated in Fig. 3, where we show that the values of the effective viscosity of suspensions with different volume fractions (placed at the intersections of blue and yellow curves, $d \approx 24$ nm) can be described using two different sets of parameters, N and ℓ, in the micropolar solution (9). In the general case, there arise infinite combinations of possible values of N and ℓ that can be identified from the experiment with the same particle size.

Thus, for unique identification of micropolar parameters, experiments need to be conducted for suspensions with different size of particles (even at constant volume fraction). In Fig. 3, it can be seen that the curves that correspond to different sets of parameters N and ℓ (blue and yellow colors) cannot be overlapped in the whole range of particle size. Moreover, they have a single intersection, so even two tests with different average sizes of particles will be enough for the identification of N and ℓ. These results can also be proved based on the formal analysis of nonlinear equations that follow from the form of presented solutions (6) and (9) for the range $0 \leq N \leq 1$ and $\ell > 0$.

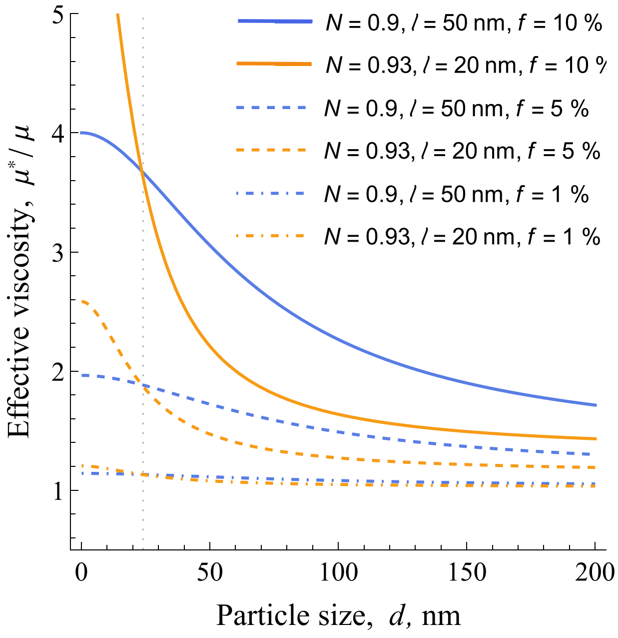

FIG. 3. Illustrations for the possible nonunique identification of micropolar parameters of size-dependent solution (9), when one considers nanofluids with different volume fractions (f) but with the same average size of particles.

In the following, we will analyze the experimental data for the viscosity of nanofluids with three or more distinct average particle sizes. The fitting will be performed by using micropolar solution for concentrated suspensions (9) using a least squares approximation. Different volume fractions of inclusions are also considered. These results are used to validate the model and to show that the identified values of N and ℓ remain unique for the considered combination of the base fluid and the particle material at different concentrations. Additionally, we consider the tests at various temperature such that the temperature-dependent micropolar parameters can be found. The value of the shear viscosity of the base fluid, μ, is also measured separately at various temperatures. This value, μ, is used in solution (9) as an input parameter along with the prescribed volume fraction, f, and average size of particles, d. Values of N and ℓ are found (identified) from the fitting procedure. Finally, the non-classical rotational viscosity, κ, and spin viscosity, γ, of the base fluid will be found (at given temperature) using the relations that follow from (10):

$$\kappa = \mu \frac{N^2}{1 - N^2}, \quad \gamma = 4\mu\ell^2. \tag{11}$$

The definition for coupling number N $(10)_1$ is generally consistent across published works in the field of micropolar theory. In contrast, there are various definitions for the length scale parameter, ranging from renormalization[16] to the utilization of inverse quantities ($\sim \ell^{-1}$).[37] Nevertheless, in the following analysis we will use the presented form of definitions (10) and (11).

Previously, identification of micropolar parameters has been performed for several kinds of liquids considering size effects for the apparent flow rate in small-scale channels.[22,25,26,53] For water, it was found that the coupling number is $N = 0.84$, while the length scale parameter has the order of 35 nm.[25] However, this value is not directly equivalent to ℓ $(10)_2$, as the authors have utilized a renormalized quantity. Nevertheless, the order ℓ for water can be assessed as several dozens of nanometers, which is in line with our results of identification (see Sec. IV).

In the present study, we will provide validation of the derived solutions and experimental identification of micropolar parameters for silicone oil based TiO_2 nanofluids. Assessments for water and ethylene glycol will also be given based on processing of the known experimental data with the other types of nanofluids.

III. MATERIALS AND METHODS USED IN EXPERIMENTAL TESTS

Suspensions were prepared by using polydimethylsiloxane (PDMS)-400 (analogue to XIAMETER PMX-200 Silicone Fluid 400 cSt) as a base fluid. PDMS-400 has a molecular weight 162.38 g/mol, density of 980 kg/m^3, kinematic viscosity at room temperature of 400 cSt, and boiling point >300 °C. This silicone oil is widely used in different applications related to oil and polymer industries and in lubricants and medicines.

The titanium dioxide nanoparticles were used as a filler. Three kinds of TiO_2 powders with average diameters of particles, $d = 47$, 114, and 386 nm, were used in the tests. In the following, these powders will be referred to as P47, P114, and P386, respectively. The powders P47 and P114 were produced using plasma-chemical synthesis,[54,55] while P386 was supplied (by TYTANPOL R-210, Grupa Azoty).

The particles size was measured by using transmission electron microscopy (TEM) and image analysis. Transmission electron microscope JEOL JEM-1400 PLUS (Akishima, Japan) was used at an accelerating voltage of 120 kV. Examples of TEM microphotographs for the used TiO_2 powders are presented in Fig. 4. TEM was performed in ethanol solution on a perforated copper substrate. In Figs. 4(a)–4(c), we show the images of the powders captured at identical magnifications to highlight the variations in particle sizes. In Figs. 4(d) and 4(e), higher magnification is used to show the shape of particles in P47 and P114 powders. It can be seen that particles have approximately spherical shape. The distributions of particle diameters obtained based on image analysis are presented in Fig. 5.

The crystalline structure of the powders was analyzed using x-ray diffractometer Aeris (Malvern Panalytical B.V., UK) equipped with a copper anode and linear detector PIXcel1D. It was found that the powders have mixed rutile/anatase composition with percentage 25/75 (P47), 46/54 (P114), and 100/0 (P386). The rutile/anatase structure may slightly affect the viscosity of nanofluids with TiO_2 fillers, although it has been shown[56] that these effects are not higher than 10%–15%. Thus, the observed strong change in viscosity in our experiments can be attributed primarily to the size effect.

The nanofluids were prepared with three volumetric concentrations of particles, $f = 1$, 2, and 5 vol. %, and three kinds of TiO_2 powders, P47, P114, and P386. In total, nine variants of nanofluid compositions were considered. The prepared suspensions were sonicated in an ultrasonic bath for 30 min at room temperature to stabilize the suspensions and to prevent the agglomeration of particles.

The viscosity of the nanofluids was measured using a RheoStress RS150 rheometer (HAAKE, Germany) with a cone spindle (cone angle 2°, gap 0.105 mm, radius 35 mm). Viscosity measurements were conducted for the shear rates 50–100 s^{-1}. In this range, the nanofluids exhibited typical Newtonian behavior. The temperature was adjusted in 10 °C increments, ranging from 20 to 60 °C, and was tracked using a HAAKE thermocontroller DC50. The required temperature was maintained during test with an accuracy of ±0.1 °C. The effective viscosity was determined by averaging the results of three repeated tests performed for the nanofluid samples of the same composition. Across all types of nanofluids, the variation in effective viscosity among the repeated tests did not exceed 7%.

IV. RESULTS AND DISCUSSION

The results of the performed tests and the fitted micropolar solution (9) for the effective viscosity of PDMS-400/TiO_2 nanofluids are presented in Figs. 6(a)–6(e). In these plots, we show all experimental data (by points) obtained at various temperatures, $T = 20$–60 °C. It can be seen that a typical positive size effect is observed: the shear viscosity of the nanofluid, μ^*, increases for smaller particles. An increase in μ^* also arises for larger volume fractions, while it decreases at higher temperature. The fitted micropolar solution (9) is shown by the curves in Figs. 6(a)–6(e). The identified values of the micropolar parameters N and ℓ are denoted on these plots. Note that these parameters are found in a least squares approximation for the set of experimental data points at given temperature. It can be seen that rather good agreement with experimental data is achieved, implying that only two additional parameters (N, ℓ) allow us to correctly describe nine experimental points for the size effect at given temperature. The mean deviation of the fitted solution from experimental points is not higher than 10% for all temperatures. For comparison, we show the results of least squares approximation of the couple stress theory [solution (9) with $N = 1$] in Fig. 6(f). It is evident that for a relatively high volume fraction of

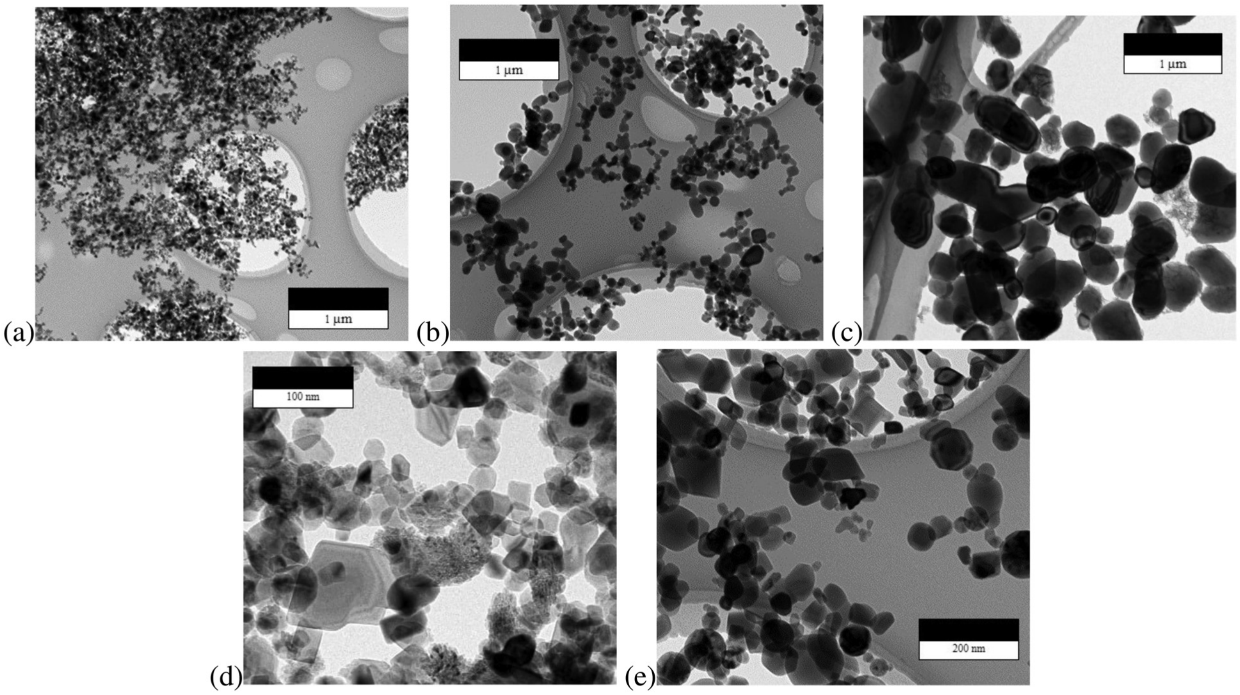

FIG. 4. TEM microphotographs of TiO_2 powders used for the preparation of nanofluids. Powders have different average diameters of particles: (a) and (d) P47 sample, $d = 47$ nm, (b) and (e) P114 sample, $d = 114$ nm, and (c) P386 sample, $d = 386$ nm.

particles [red curve in Fig. 6(f)], the couple stress solution cannot be precisely matched with the experimental data unless some additional assumptions are incorporated for the remaining model parameter ℓ.

The identified values of micropolar parameters are collected in Fig. 7(a). It can be seen that the coupling number, N, of PDMS-400 remains almost independent of temperature and takes values in the range $0.972 - 0.976$. The identified length scale parameter has value $\ell \approx 140$ nm at room temperature and approximately 10% increase for the highest testing temperature $T = 60\,^{\circ}$C. The viscosity properties of PDMS-400 are presented in Fig. 7(b). The blue line here corresponds to the values of standard shear viscosity, μ, that was measured for PDMS-400 without nanoparticles. The presented values of non-classical rotational viscosity, κ, and spin viscosity, γ [red and yellow curves in Fig. 7(b)] are evaluated by using the identified values of micropolar parameters N and ℓ [Fig. 7(a)] and formulas (11). It is notable that all viscosity coefficients μ, κ, and γ decrease for higher temperature, though some non-monotonic dependences are observed for parameters N and ℓ. The rotational viscosity, κ, of PDMS-400 is about one order higher than its shear viscosity, μ. The spin viscosity, γ, has a different dimension, and its values lie in the range 22–32 kPa s nm^2.

In Fig. 7, we also give the uncertainties in the fitted data/curve. To evaluate the uncertainties, we took the subsets of experimental data points with the same volume fraction and different size of particles. For each subset, we found the values of the micropolar parameters based on the fitting of solution (9). In this way, we found the dependence of the

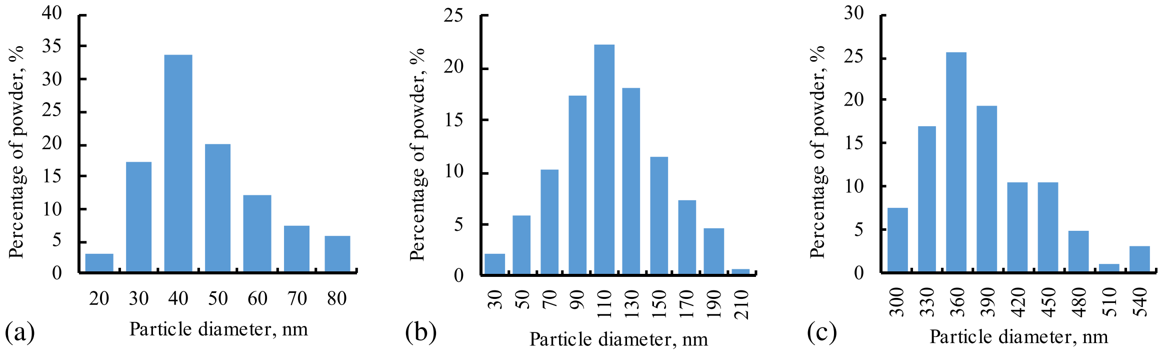

FIG. 5. Distribution of particle diameters in TiO_2 powders P47 (a), P114 (b), and P386 (c).

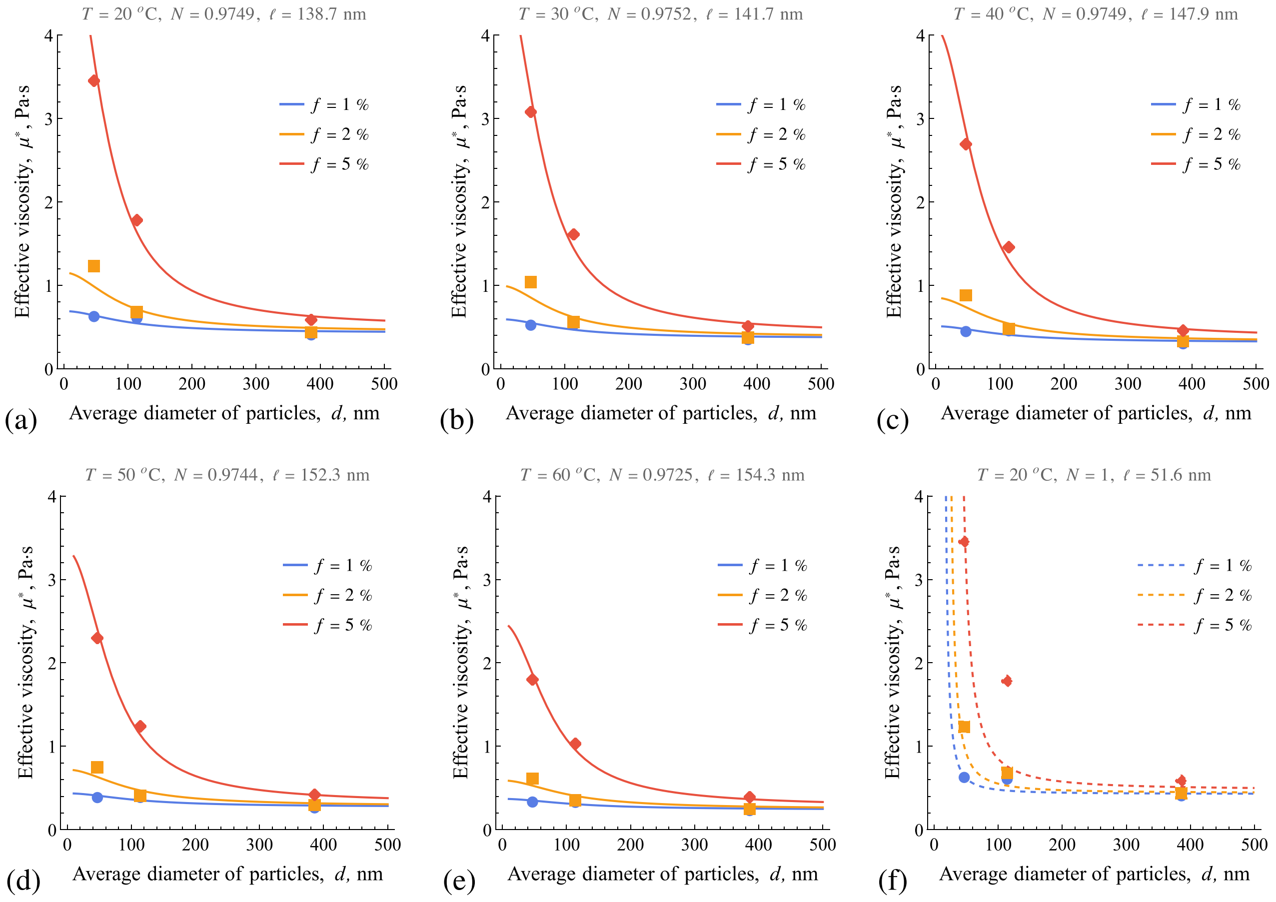

FIG. 6. Dependence of the effective shear viscosity of PDMS-400/TiO_2 nanofluids on the average size of particles, volume fraction, and temperature. Points—experimental data. Lines—fitted micropolar solution (9). Identified micropolar parameters are denoted on the plots. (a) $T = 20$, (b) $T = 30$, (c) $T = 40$, (d) $T = 50$, (e) $T = 60\,°C$, and (f) example of fitting of couple stress theory ($N = 1$) for $T = 20\,°C$.

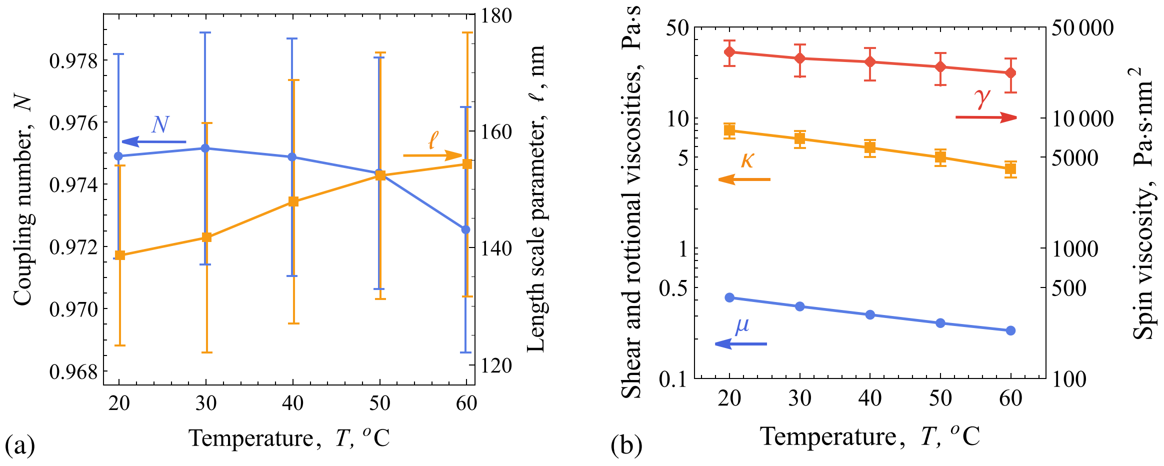

FIG. 7. (a) Identified temperature-dependent values of micropolar model parameters of PDMS-400. (b) Temperature-dependent shear viscosity μ, rotational viscosity κ, and spin viscosity γ of PDMS-400.

TABLE I. Properties of the base fluids determined by fitting of micropolar solutions to the experimental data for the shear viscosity of nanofluids.

Base fluid	Particles	T (°C)	N	ℓ (nm)	μ (mPa s)	κ (mPa s)	γ (Pa s nm^2)	Source
PDMS-400	TiO_2 (1%–5%)	20	0.9749	138.7	420	8000	32 100	This work
		30	0.9752	141.7	360	6900	28 600	
		40	0.9749	147.9	310	5900	26 900	
		50	0.9744	152.3	270	5000	24 600	
		60	0.9725	154.3	230	4100	22 100	
Ethylene glycol	Fe (0.5%–3%)	26	0.8834	46.73	19.5	69.3	170.3	Ref. 41
		35	0.89	36.9	11.2	42.7	61.1	
		45	0.9031	31.19	8.3	36.7	32.3	
		55	0.8741	38.7	5.2	16.8	31.2	
Water, pH 5.5	SiO_2 (0.1%–2%)	25	0.9755	18	0.9	17.7	1.2	Ref. 42
Water, pH 9.4	SiC (4.1%)	15	0.9198	18.8	1.15	6.3	1.6	Ref. 43
		25	0.9182	23.8	0.9	4.8	2.0	
		35	0.9180	25.0	0.72	3.9	1.8	
		45	0.9323	19.1	0.6	4.0	0.88	
		55	0.9320	17.0	0.5	3.3	0.58	

identified micropolar parameters on the volume fraction of particles. Then, we calculated the mean value and standard deviation of the identified micropolar parameters across all subsets. The mean values were close to our initial results of identification, which were performed for the whole set of data points (for all volume fractions and particle sizes). The standard deviations were used to define the uncertainties (error bars) in plots in Fig. 7. The same approach is applied below for the plots in Fig. 10.

All the temperature-dependent parameters of the micropolar model for PDMS-400 are collected in Table I. In this table, we also give the identified parameters of ethylene glycol and water that we obtained based on the processing of experimental data for the other kinds of nanofluids taken from Refs. 41–43.

The data for ethylene glycol based nanofluid with Fe nanoparicles were taken from Ref. 41. In this paper, the authors found the dependence of the shear viscosity of nanofluid on volume fraction, particle size, and temperature. The processing of these experimental data with the micropolar model (9) is illustrated in Figs. 8 and 9. In Fig. 8(a), we show the experimental data points and the fitted curves of solution for different temperature conditions. Good agreement is obtained for all the data points, while the absolute values of the effective viscosity of these nanofluids is two orders lower than in our PDMS-400 based nanofluids. This means that the presented solutions can also be applied to the suspensions with relatively low viscosity. Note that for each temperature, we found unique values of micropolar parameters N and ℓ and used them to plot the curves in Fig. 8(a). The identified values of

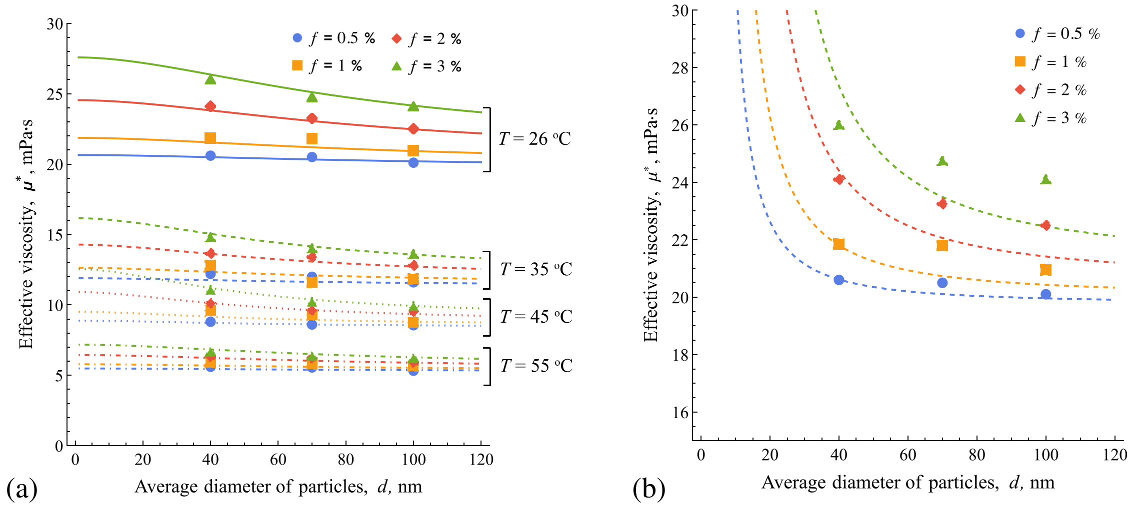

FIG. 8. (a) Dependence of the effective shear viscosity of ethylene glycol/Fe nanofluids on average size of particles, volume fraction, and temperature. Points—experimental data from Ref. 41. Lines—fitted micropolar solution (9). (b) Example of fitting of couple stress theory ($N = 1$) for $T = 26\,°C$.

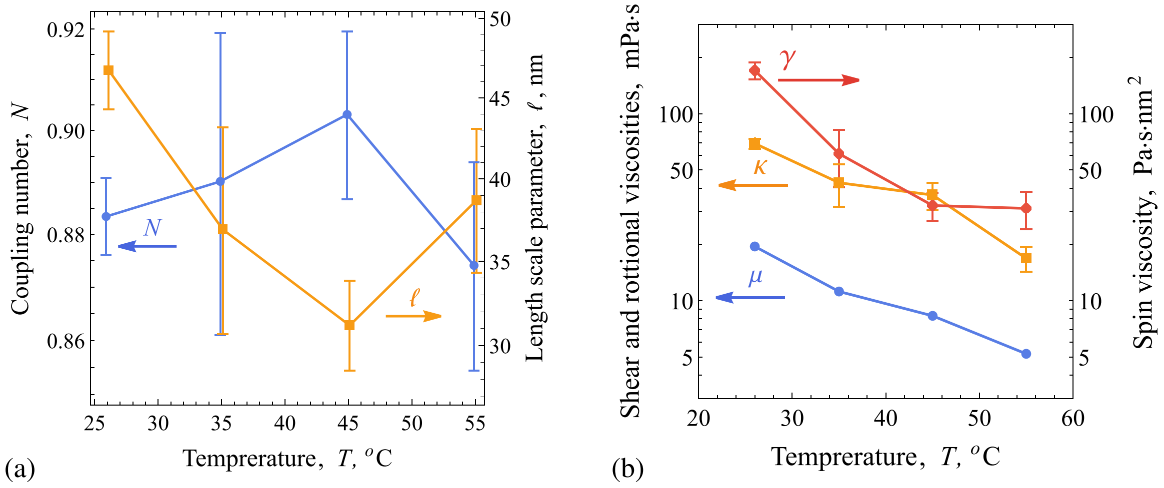

FIG. 9. (a) Identified temperature-dependent values of micropolar model parameters of ethylene glycol. (b) Temperature-dependent shear viscosity μ, rotational viscosity κ, and spin viscosity γ of ethylene glycol.

these parameters and related values of the non-classical rotational and shear viscosities (11) of ethylene glycol are presented in Fig. 9 and in Table I. The values of standard shear viscosity of ethylene glycol that were used in calculations are marked by a blue line in Fig. 9(b). An example of fitting of the couple stress theory (with unit value of coupling number, $N = 1$) for the nanofluid properties at $T = 26\,^\circ$C is given in Fig. 8(b). It can be seen that, similar to our experiments with PDMS-400/TiO$_2$ [Fig. 6(f)], this high-grade theory cannot be used for suspensions with relatively high volume fractions of particles.

The data for the water based nanofluids with SiO$_2$ particles were taken from Ref. 42. In this work, the authors used the de-ionized water (pH 5.5) and presented the results of viscosity measurements for nanofluids with different sizes (7–40 nm) and volume fractions of particles (up to 2%) at room temperature ($T = 25\,^\circ$C). A comparison of the experimental data with the Brinkman's micropolar formula (9) is given in Fig. 10. Comparison with the corresponding couple stress solution (with $N = 1$) is given in Fig. 10(b). It is seen that the micropolar model provides accurate description of experimental data in the whole range of volume fractions and size of particles. The identified micropolar parameters for de-ionized water are $N = 0.9755 \pm 0.0056$ and $\ell = 18 \pm 2.9$ nm (the standard deviation is evaluated as discussed above). The related values of non-classical viscosities estimated by using relations (11) are given in Table I.

The last considered set of experimental results was taken from Ref. 43, where the authors investigated the viscosity of water based nanofluids with 0.22 vol. % SiC particles of different sizes and at

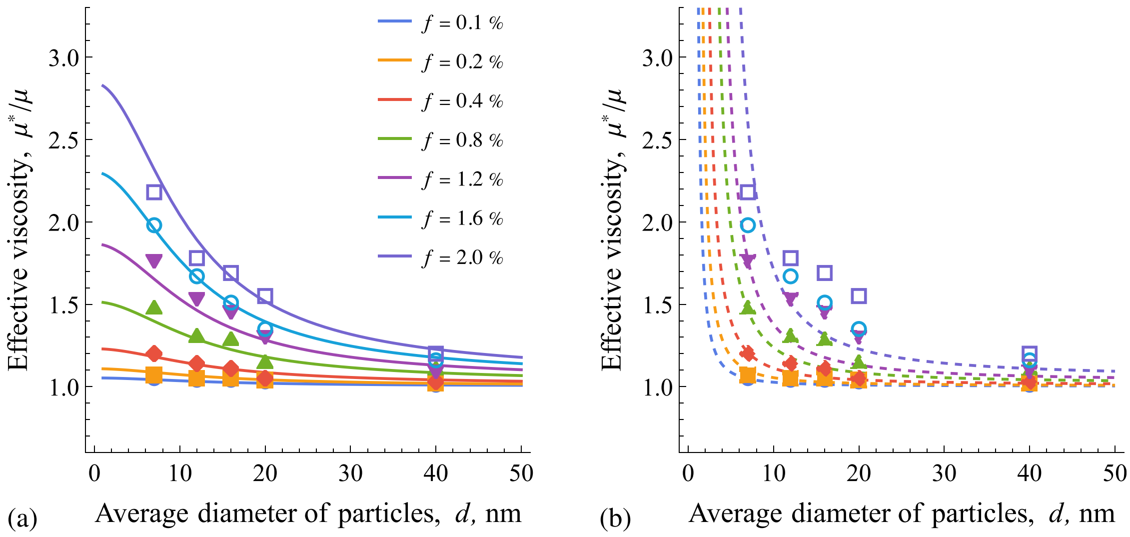

FIG. 10. (a) Dependence of the effective shear viscosity of water/SiO$_2$ nanofluids on average size and volume fraction of particles. Points—experimental data from Ref. 42. Lines—fitted micropolar solution (9). (b) Example of fitting of the couple stress theory ($N = 1$).

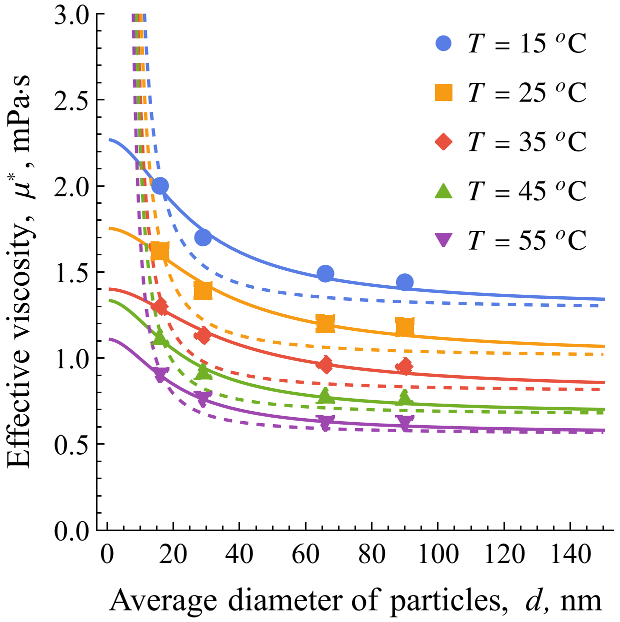

FIG. 11. Dependence of the effective shear viscosity of water/SiC nanofluids on average size of particles and temperature. Points—experimental data from Ref. 43. Solid lines—fitted micropolar solution (9). Examples of fitting of couple stress theory ($N = 1$) are shown by dashed lines.

different temperatures. The authors used distilled water and adjusted its pH level up to 9.4 using solutions of ammonium hydroxide. The fitted micropolar solution to these data is given in Fig. 11. It can be seen that the two-parametric solution allows us to describe the whole experimental data with high accuracy (solid lines in Fig. 11). The identified temperature-dependent micropolar parameters of water are given in Fig. 12 and also in Table I. It can be seen that, similar to our previous results, the classical and non-classical viscosities have a tendency to decrease at higher temperature. Note that the error bars are not shown in Fig. 12 as only a single value of the volume fraction was considered in these tests. Consequently, it is not possible to estimate the standard deviations among the identification results for different volume fractions as suggested above. At the same time, from Fig. 12(a), it is seen that the micropolar parameters do not exhibit significant variation with changes in temperature ($N = 0.924 \pm 0.0075$ and $\ell = 20.7 \pm 3.5$ for $T = 15$–$55\,°$C).

Now, we can compare the identified values of the micropolar parameters of different fluids. From Table I, one can see that the highest value of the length scale parameter has silicone oil PDMS-400 ($\ell \approx 145$ nm), while the ethylene glycol has a smaller value ($\ell \approx 40$ nm) and the smallest is found for water ($\ell \approx 20$ nm). This can be attributed to the molar mass of these fluids, which are 162.38 g/mol (PDMS-400), 62.07 g/mol (ethylene glycol), and 18.01 g/mol (water), respectively. Therefore, we can suppose that the length scale parameter is larger in fluids with higher molar mass, where the larger molecular aggregates (or polymer chains) make the micropolar effects more pronounced. Generally, the higher values of the length scale parameter can also be attributed to the stronger adhesion interactions existing between the fluid and the solid particles.[15] For the coupling number, there are no such obvious dependencies. We can only note that the found rotational viscosity, κ, is 5–20 times higher than the classical shear viscosity, μ, for all the considered fluids (see Table I). This rotational viscosity defines the coupling number, N [see (10)], which took values of about 0.9–0.98 in all the considered tests. Perhaps, the values of N are influenced by the pH level and polarity of the liquid, as well as the zeta potential of the particles, but this requires additional research.

Note that the identified micropolar parameters of water, found from different experimental tests from Refs. 42 and 43, are rather close to each other and to the previously known results.[25] The experiments with nanofluids[42,43] were performed with different kinds of particles and at different pH levels. Nevertheless, from Table I, it is seen that the values for the length scale parameter at room temperature are very close for both the tests: $\ell \approx 20$ nm. The coupling number has values ~0.97 and ~0.92 in these experiments, which can be related, e.g., to

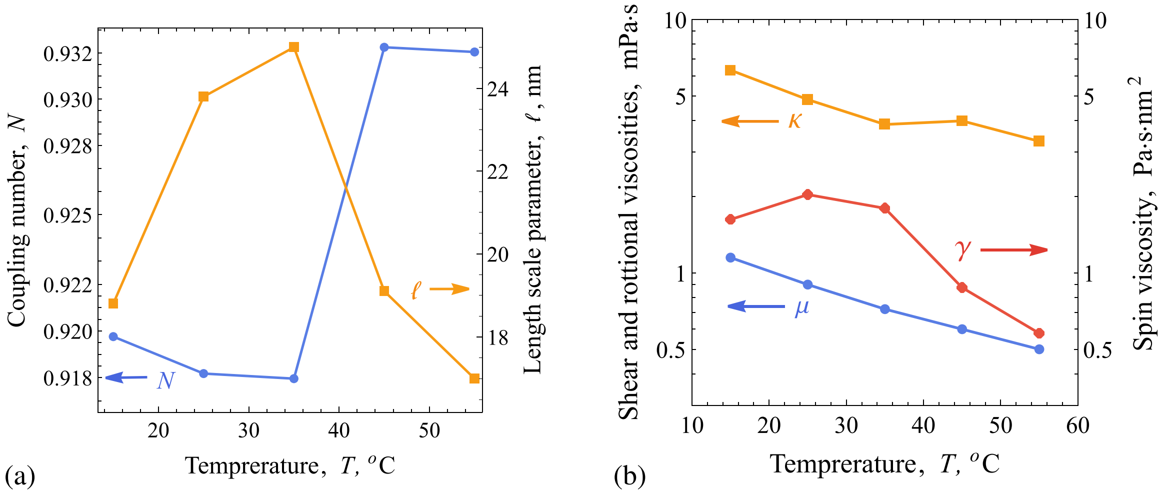

FIG. 12. Identified temperature-dependent values of micropolar model parameters (a) and shear viscosity μ, rotational viscosity κ, and spin viscosity γ (b) of distilled water (pH 9.4).

the change in pH level (from 5.5 to 9.4, respectively). As a result of nonlinear relation between N and κ (11), the latter shows much stronger change and its values become three times smaller at higher pH 9.4. The previously reported micropolar properties of water were $N = 0.84$ and $\ell' = 35\,\text{nm}$.[25] In the present study, we identified somewhat higher values for the coupling number, while the length scale parameter has the same order. We can evaluate the value of ℓ' following its definition used in Ref. 25: $\ell' = \sqrt{\frac{\gamma}{\kappa}\frac{\mu+\kappa}{2\mu+\kappa}}$. By using established values of viscosities μ, κ, and γ (Table I), we found that this re-normalized length scale parameter at $T = 25\,^{\circ}\text{C}$ takes the value $\ell' = 7.9$ [de-ionized water, pH 5.5 (Ref. 42)] and $\ell' = 18$ [distilled water, pH 9.4 (Ref. 43)]. Therefore, the identified micropolar properties of distilled water are closer to those presented in Ref. 25, where the identification was performed based on the analysis of apparent flow rate in small-scale channels. Note that these results can also be influenced by the scattering and uncertainties of experimental data as well as the characteristics of the solid material (channel walls).

Regarding temperature effects, we can note that all viscosity coefficients, μ, κ, and γ, decrease with increasing temperature. However, this effect is primarily associated with decrease in the classical shear viscosity, μ. As indicated by relations (11), the non-classical coefficients κ and γ are proportional to μ, and therefore they also decrease with increasing temperature. The impact of temperature effects on the micropolar parameters, which persist in the dimensionless formulation of the model (N and ℓ), cannot be unambiguously identified based on the available data due to the influence of identification uncertainties [see Figs. 7(a) and 9(a)]. It can only be stated that the variation of parameters N and ℓ is relatively small compared to the relative change in the classical viscosity coefficient μ.

V. CONCLUSION

In this paper, we propose a new variant of size-dependent solutions for the effective viscosity of rigid particle suspensions. We show that these solutions allow to describe the experimental data on the dependence of the nanofluid's effective viscosity on the volume fraction and average size of particles. We show that accurate description of the size effects can be obtained by using two additional non-classical parameters: the coupling number and the length scale parameter. These micropolar properties of the base fluids are identified based on the performed tests with PDMS-400/TiO_2 nanofluid and based on the known data for ethylene glycol/Fe, water/SiO_2, and water/SiC nanofluids. Temperature-dependent values of non-classical rotational and spin viscosities are also assessed. It is shown that these viscosities as well as the classical shear viscosity of the base fluid have a tendency to decrease with increase in temperature. For the previously derived solutions within the couple stress theory,[39] it is shown that it can be used for the relatively small volume fractions of inclusions, while the micropolar effects cannot be ignored for the more concentrated nanofluids with $f > 2\%$.

Future works should be related to the analysis of a wider class of nanofluids with more data points for different volume fractions and size of particles. The influence of particle material and the surface state of the particles on the identified micropolar properties of the base fluids should be investigated. The influence of particle size distribution and possible agglomeration effects should be included in the theoretical analysis.

ACKNOWLEDGMENTS

This work was performed with the support of the Russian Science Foundation Grant No. 23-11-00275 issued to IAM RAS (for model, testing, analysis) and within the framework of state Assignment No. 124013000757-0 in FRC PCP MC RAS (for powder production).

AUTHOR DECLARATIONS

Conflict of Interest

The authors have no conflicts to disclose.

Author Contributions

R. Bondarenko: Data curation (equal); Formal analysis (equal); Writing – review & editing (equal). **Yu. Bukichev:** Investigation (equal); Resources (equal); Writing – review & editing (equal). **A. Dzhaga:** Data curation (equal); Investigation (equal); Visualization (equal); Writing – review & editing (equal). **G. Dzhardimalieva:** Methodology (equal); Resources (equal); Supervision (equal); Writing – review & editing (equal). **Y. Solyaev:** Conceptualization (equal); Investigation (equal); Methodology (equal); Software (equal); Writing – original draft (equal).

DATA AVAILABILITY

The data that support the findings of this study are available from the corresponding author upon reasonable request.

APPENDIX A: ANALOGY BETWEEN THE MICROPOLAR THEORIES OF INCOMPRESSIBLE SOLIDS AND FLUIDS

For the steady-state processes in the absence of body forces, the balance equations for the liner momentum and angular momentum within the micropolar theory are given by[16,57]

$$\begin{aligned} \nabla \cdot \boldsymbol{\sigma} &= 0, \\ \nabla \cdot \boldsymbol{\mu} + \boldsymbol{\sigma}_{\times} &= 0, \end{aligned} \tag{A1}$$

where $\boldsymbol{\sigma}$ is the (nonsymmetric) stress tensor, $\boldsymbol{\mu}$ is the couple stress tensor, $\boldsymbol{\sigma}_{\times}$ is the axial vector associated with the skew-symmetric part of the stress tensor $\boldsymbol{\sigma}$, ∇ is the spatial nabla operator.

The field equations (A1) remain valid for the solids and fluids.[57] The constitutive equations for the incompressible micropolar media can also be defined in a unified form as follows:[16,37,57]

$$\begin{aligned} \boldsymbol{\sigma} &= -p\boldsymbol{I} + (\mu + \kappa)\boldsymbol{\varepsilon} + (\mu - \kappa)\boldsymbol{\varepsilon}^T, \\ \boldsymbol{\mu} &= \alpha \nabla \cdot \boldsymbol{\omega} \boldsymbol{I} + \gamma \nabla \boldsymbol{\omega} + \beta (\nabla \boldsymbol{\omega})^T, \end{aligned} \tag{A2}$$

where p is the hydrostatic pressure, $\boldsymbol{I}$ is the second order identity tensor, and within the micropolar theory of fluids (solids) $\boldsymbol{\varepsilon} = \nabla \boldsymbol{v} + \boldsymbol{I} \times \boldsymbol{\omega}$ is the measure for strain rate (strain), $\boldsymbol{v}$ is the linear velocity field (the displacement field), $\boldsymbol{\omega}$ is the angular velocity field (rotation vector), μ is the standard shear viscosity (shear modulus), and κ, α, β, γ are the additional viscosity (elastic) properties of micropolar fluid (solid). The incompressibility condition implies that $\nabla \cdot \boldsymbol{v} = 0$.

Substituting (A2) into (A1), one can obtain the motion equations in terms of kinematic variables and pressure:

$$\begin{aligned}&(\mu+\kappa)\nabla^2\boldsymbol{v}+2\kappa\nabla\times\boldsymbol{\omega}=\nabla p,\\&(\alpha+\beta)\nabla\nabla\cdot\boldsymbol{\omega}+\gamma\nabla^2\boldsymbol{\omega}-4\kappa\left(\boldsymbol{\omega}-\frac{1}{2}\nabla\times\boldsymbol{v}\right)=0.\end{aligned}\tag{A3}$$

Boundary conditions can be prescribed with respect to the linear $\boldsymbol{u}$ and angular $\boldsymbol{\omega}$ velocity of fluid (displacements and rotations in solids) or with respect to the normal components of stress $\boldsymbol{n}\cdot\boldsymbol{\sigma}$ and couple stress $\boldsymbol{n}\cdot\boldsymbol{\mu}$. Mixed boundary conditions are also allowable.[57] Continuity conditions should be prescribed with respect to all the mentioned quantities.

In the theory of micropolar fluids, the non-classical coefficient κ is denoted as the rotational viscosity[16,24] (or vortex viscosity[20]). It can be seen that nonzero values of this coefficient provides the coupling between the balance equations for the linear and angular momentum in (A3). The non-classical coefficients α, β, γ are denoted as spin viscosity[24] (or couple viscosities,[20] viscosities of the gradient of total rotation,[16] angular viscosities,[22] etc.). In some references,[19] authors use modified definitions for these coefficients, such as $\gamma\leftrightarrow(\gamma+\beta)$ and $\beta\leftrightarrow(\gamma-\beta)$. The present notation is more useful for the considered problems because it allows us to find the coefficient γ (instead of the sum $\gamma+\beta$) in the main part of the paper.

Statements (A1)–(A3) are equivalent to those used in the initial works on micropolar micromechanics,[37] where the explicit solution for the Eshelby tensor for the spherical inclusion problem has been obtained. The single difference is that we use double value of the coefficient κ (to obtain exact match with Ref. 37, one should replace $\kappa\to\kappa/2$). In this way, we obtain a definition for the coupling number, $N=\sqrt{\kappa/(\mu+\kappa)}$ (10) [instead of $N=\sqrt{\kappa/(2\mu+\kappa)}$], that is more common in micropolar fluids mechanics.[16,22] Using this relation and those used for the length scale parameter $\ell=\sqrt{\gamma/(4\mu)}$ (10), we can reduce (A3) to the following non-dimensional form:[37]

$$\begin{aligned}&\frac{1+N^2}{1-N^2}\frac{1}{\mathrm{Re}}\nabla^2\boldsymbol{v}'+\frac{2N^2}{1-N^2}\frac{1}{\mathrm{Re}}\nabla\times\boldsymbol{\omega}'=\nabla p',\\&\frac{\ell_\alpha^2+\ell_\beta^2}{L^2}\nabla\nabla\cdot\boldsymbol{\omega}'+\frac{\ell^2}{L^2}\nabla^2\boldsymbol{\omega}'-\frac{N^2}{1-N^2}\left(\boldsymbol{\omega}'-\frac{1}{2}\nabla\times\boldsymbol{v}'\right)=0,\end{aligned}\tag{A4}$$

where the non-dimensional field variables are defined by $\boldsymbol{v}'=\boldsymbol{v}/V$, $\boldsymbol{\omega}'=L\ \boldsymbol{\omega}/V$, $p'=p/(\rho V^2)$; L and V are the characteristic length and velocity of the problem, respectively; ρ is the mass density; $\mathrm{Re}=\rho VL/\mu$ is the Reynolds number; $\ell_\alpha=\sqrt{\alpha/(4\mu)}\geq 0$, $\ell_\beta=\sqrt{\beta/(4\mu)}\geq 0$ are the length scale parameters that are related to the corresponding spin viscosities.

Among four non-classical parameters of micropolar theory (N, ℓ, ℓ_α, and ℓ_β), only two (N and ℓ) arise in the solution for the effective shear viscosity (shear modulus) for media with spherical inhomogeneities. These parameters together with the related rotational viscosity, κ, and spin viscosity, γ, were identified in the main part of the paper.

APPENDIX B: SOLUTION FOR THE COMPONENT OF THE ESHELBY TENSOR S_{1212}

Solution for the component of the Eshelby tensor S_{1212} (4) was derived in Ref. 37 for compressible micropolar media in the following form:

$$S_{1212}=\frac{3(K+2\mu)}{5(3K+4\mu)}-\frac{3h(a+h)\kappa}{5a^3(\kappa+\mu)}\mathrm{e}^{-a/h}\left(a\cosh\frac{a}{h}-h\sinh\frac{a}{h}\right),\tag{B1}$$

where we replace κ by 2κ as mentioned above; $h=\sqrt{\gamma(\mu+\kappa)/(4\mu\kappa)}=\ell/N$ is the modified definition for the length scale parameter used in Ref. 37; a is radius of spherical inclusion; K, μ, κ, γ are the bulk modulus, shear modulus, and micropolar parameters of matrix media, respectively.

Using standard relations between the engineering constants K, μ, ν and taking into account our definitions for N and ℓ (10) in (B1), one can obtain

$$S_{1212}=\frac{4-5\nu}{15(1-\nu)}+\frac{3}{5}\,\frac{N^2(1+a/h)}{(a/h)^3}\mathrm{e}^{-a/h}\left(\frac{a}{h}\cosh\frac{a}{h}-\sinh\frac{a}{h}\right).\tag{B2}$$

Introducing the normalized diameter of spherical particle $\bar{d}=2Na/\ell$ and providing standard algebraic simplifications in Eq. (B2), one can obtain the form of S_{1212} that was given in Eq. (4). For the limiting case of incompressible media ($\nu\to 0.5$), we obtain then the form of the Eshelby tensor component (5) that corresponds to the statement of micropolar theory (A1)–(A4). Therefore, representation (5) is valid (up to notations) for micropolar incompressible solids and fluids (at low Reynolds number).

REFERENCES

[1] G. F. Smaisim, D. B. Mohammed, A. M. Abdulhadi, K. F. Uktamov, F. H. Alsultany, S. E. Izzat, M. J. Ansari, H. H. Kzar, M. E. Al-Gazally, and E. Kianfar, "Nanofluids: Properties and applications," J. Sol-Gel Sci. Technol. **104**, 1–35 (2022).

[2] H. D. Koca, S. Doganay, A. Turgut, I. H. Tavman, R. Saidur, and I. M. Mahbubul, "Effect of particle size on the viscosity of nanofluids: A review," Renewable Sustainable Energy Rev. **82**, 1664–1674 (2018).

[3] F. Jabbari, A. Rajabpour, and S. Saedodin, "Thermal conductivity and viscosity of nanofluids: A review of recent molecular dynamics studies," Chem. Eng. Sci. **174**, 67–81 (2017).

[4] J. P. Meyer, S. A. Adio, M. Sharifpur, and P. N. Nwosu, "The viscosity of nanofluids: A review of the theoretical, empirical, and numerical models," Heat Transfer Eng. **37**, 387–421 (2016).

[5] M. Klazly and G. Bognár, "A novel empirical equation for the effective viscosity of nanofluids based on theoretical and empirical results," Int. Commun. Heat Mass Transfer **135**, 106054 (2022).

[6] C. Ezekwem, "A recent review of viscosity models for nanofluids," Energy Sources, Part A **44**, 1250–1315 (2022).

[7] A. Abdelrazik, M. A. Sayed, A. Mahmoud, F. A. FM, H. Alshimaa, A. Oulguidoum, E. Kotob, and M. H. Helmy, "Potential of molecular dynamics in the simulation of nanofluids properties and stability," J. Mol. Liq. **381**, 121757 (2023).

[8] J. M. Munyalo and X. Zhang, "Particle size effect on thermophysical properties of nanofluid and nanofluid based phase change materials: A review," J. Mol. Liq. **265**, 77–87 (2018).

[9] W. Yu and S. Choi, "The role of interfacial layers in the enhanced thermal conductivity of nanofluids: A renovated Hamilton–crosser model," J. Nanopart. Res. **6**, 355–361 (2004).

[10] Z. Lou and M. Yang, "Molecular dynamics simulations on the shear viscosity of Al_2O_3 nanofluids," Comput. Fluids **117**, 17–23 (2015).

[11] G. Lu, Y.-Y. Duan, and X.-D. Wang, "Surface tension, viscosity, and rheology of water-based nanofluids: A microscopic interpretation on the molecular level," J. Nanopart. Res. **16**, 2564 (2014).

[12] H. Xie, M. Fujii, and X. Zhang, "Effect of interfacial nanolayer on the effective thermal conductivity of nanoparticle-fluid mixture," Int. J. Heat Mass Transfer **48**, 2926–2932 (2005).

[13] S. Masoud Hosseini, A. Moghadassi, and D. Henneke, "A new dimensionless group model for determining the viscosity of nanofluids," J. Therm. Anal. Calorim. **100**, 873–877 (2010).

[14] J. Dahler and L. Scriven, "Angular momentum of continua," Nature **192**, 36–37 (1961).

[15] A. C. Eringen, "Theory of micropolar fluids," J. Math. Mech. **16**, 1–18 (1966), https://www.jstor.org/stable/24901466.

[16] S. Cowin, "The theory of polar fluids," Adv. Appl. Mech. **14**, 279–347 (1974).

[17] D. W. Condiff and J. S. Dahler, "Fluid mechanical aspects of antisymmetric stress," Phys. Fluids **7**, 842–854 (1964).

[18] G. Lukaszewicz, *Micropolar Fluids: Theory and Applications* (Springer Science & Business Media, 2012).

[19] W. Rickert, E. Vilchevskaya, and W. Müller, "A note on Couette flow of micropolar fluids according to Eringen's theory," Math. Mech. Complex Syst. **7**, 25–50 (2019).

[20] K. P. Travis and D. Evans, "Molecular spin in a fluid undergoing Poiseuille flow," Phys. Rev. E **55**, 1566 (1997).

[21] J. Chen, C. Liang, and J. Lee, "Theory and simulation of micropolar fluid dynamics," Proc. Inst. Mech. Eng., Part N **224**, 31–39 (2010).

[22] D. Y. Khanukaeva and A. Troshkin, "Steady nanocapillary flow: Micropolar approach vs classical models," Phys. Fluids **35**, 072005 (2023).

[23] G. Sofiadis and I. Sarris, "Microrotation viscosity effect on turbulent micropolar fluid channel flow," Phys. Fluids **33**, 095126 (2021).

[24] J. S. Hansen, P. J. Daivis, J. C. Dyre, B. Todd, and H. Bruus, "Generalized extended Navier-Stokes theory: Correlations in molecular fluids with intrinsic angular momentum," J. Chem. Phys. **138**, 034503 (2013).

[25] V. Kolpashchikov, N. Migun, and P. Prokhorenko, "Experimental determination of material micropolar fluid constants," Int. J. Eng. Sci. **21**, 405–411 (1983).

[26] I. Papautsky, J. Brazzle, T. Ameel, and A. B. Frazier, "Laminar fluid behavior in microchannels using micropolar fluid theory," Sens. Actuators, A **73**, 101–108 (1999).

[27] V. K. Stokes, "Effects of couple stresses in fluids on the creeping flow past a sphere," Phys. Fluids **14**, 1580–1582 (1971).

[28] K.-H. Hoffmann, D. Marx, and N. D. Botkin, "Drag on spheres in micropolar fluids with non-zero boundary conditions for microrotations," J. Fluid Mech. **590**, 319–330 (2007).

[29] A. Einstein, "Eine neue bestimmung der moleküldimensionen," Ph.D. thesis (ETH Zurich, 1905).

[30] H. C. Brinkman, "The viscosity of concentrated suspensions and solutions," J. Chem. Phys. **20**, 571–571 (1952).

[31] M. Erdogan, "Dynamics of polar fluids," Acta Mech. **15**, 233–253 (1972).

[32] A. Avudainayagam, "The effective viscosity of a dilute suspension of micropolar fluid particles in a viscous fluid," Int. J. Eng. Sci. **14**, 703–712 (1976).

[33] R. Niefer and P. Kaloni, "Motion of a rigid sphere in a shear field in a micropolar fluid," Int. J. Eng. Sci. **19**, 959–966 (1981).

[34] M. Erdoğan, "Polar effects in the apparent viscosity of a suspension," Rheol. Acta **9**, 434–438 (1970).

[35] S. Cowin, "Polar fluids," Phys. Fluids **11**, 1919–1927 (1968).

[36] Z.-Q. Cheng and L.-H. He, "Micropolar elastic fields due to a spherical inclusion," Int. J. Eng. Sci. **33**, 389–397 (1995).

[37] X. Liu and G. Hu, "A continuum micromechanical theory of overall plasticity for particulate composites including particle size effect," Int. J. Plast. **21**, 777–799 (2005).

[38] R. M. Christensen, *Mechanics of Composite Materials* (Courier Corporation, 2012).

[39] Y. Solyaev, S. Lurie, and N. Semenov, "Generalized Einstein's and Brinkman's solutions for the effective viscosity of nanofluids," J. Appl. Phys. **128**, 035102 (2020).

[40] E. Fried and M. E. Gurtin, "Tractions, balances, and boundary conditions for nonsimple materials with application to liquid flow at small-length scales," Arch. Ration. Mech. Anal. **182**, 513–554 (2006).

[41] M. H. Esfe, S. Saedodin, O. Mahian, and S. Wongwises, "Efficiency of ferromagnetic nanoparticles suspended in ethylene glycol for applications in energy devices: Effects of particle size, temperature, and concentration," Int. Commun. Heat Mass Transfer **58**, 138–146 (2014).

[42] Z. Jia-Fei, L. Zhong-Yang, N. Ming-Jiang, and C. Ke-Fa, "Dependence of nanofluid viscosity on particle size and pH value," Chin. Phys. Lett. **26**, 066202 (2009).

[43] E. V. Timofeeva, D. S. Smith, W. Yu, D. M. France, D. Singh, and J. L. Routbort, "Particle size and interfacial effects on thermo-physical and heat transfer characteristics of water-based α-SiC nanofluids," Nanotechnology **21**, 215703 (2010).

[44] J. Aboudi, S. M. Arnold, and B. A. Bednarcyk, *Micromechanics of Composite Materials: A Generalized Multiscale Analysis Approach* (Butterworth-Heinemann, 2013).

[45] T. Mura, *Micromechanics of Defects in Solids* (Springer Science & Business Media, 2013).

[46] H. Ma and X.-L. Gao, "A new homogenization method based on a simplified strain gradient elasticity theory," Acta Mech. **225**, 1075–1091 (2014).

[47] Y. Solyaev, "Self-consistent assessments for the effective properties of two-phase composites within strain gradient elasticity," Mech. Mater. **169**, 104321 (2022).

[48] H. Duan, J. Wang, Z. Huang, and B. L. Karihaloo, "Eshelby formalism for nano-inhomogeneities," Proc. R Soc. A **461**, 3335–3353 (2005).

[49] P. Sharma and A. Dasgupta, "Average elastic fields and scale-dependent overall properties of heterogeneous micropolar materials containing spherical and cylindrical inhomogeneities," Phys. Rev. B **66**, 224110 (2002).

[50] S. Lurie, Y. Solyaev, and K. Shramko, "Comparison between the Mori-Tanaka and generalized self-consistent methods in the framework of anti-plane strain inclusion problem in strain gradient elasticity," Mech. Mater. **122**, 133–144 (2018).

[51] H. Reda, N. Mawassy, J. Aranda-Ruiz, D. Garcia-Gonzalez, and J. Ganghoffer, "Homogenization of magnetoelastic heterogeneous solid bodies based on micropolar magnetoelasticity," Continuum Mech. Thermodyn. **34**, 1641–1668 (2022).

[52] H. C. Weng, C.-K. Chen, and M.-H. Chang, "Magnetoviscosity in magnetic fluids: Testing different models of the magnetization equation," Smart Sci. **1**, 51–58 (2013).

[53] C. Kang and A. Eringen, "The effect of microstructure on the rheological properties of blood," Bull. Math. Biol. **38**, 135–159 (1976).

[54] V. Berestenko, V. Torbov, V. Chukalin, E. Kurkin, I. Balikhin, I. Domashnev, V. Troitskii, and S. Gurov, "Microwave-assisted chloride process for the production of titanium dioxide," High Energy Chem. **45**, 434–438 (2011).

[55] Y. S. Bukichev, L. M. Bogdanova, V. A. Lesnichaya, N. V. Chukanov, N. D. Golubeva, and G. I. Dzhardimalieva, "Mechanical and thermophysical properties of epoxy nanocomposites with titanium dioxide nanoparticles," Appl. Sci. **13**, 4488 (2023).

[56] D. Cabaleiro, M. J. Pastoriza-Gallego, C. Gracia-Fernández, M. M. Piñeiro, and L. Lugo, "Rheological and volumetric properties of TiO_2-ethylene glycol nanofluids," Nanoscale Res. Lett. **8**, 286 (2013).

[57] V. A. Eremeyev, M. J. Cloud, and L. P. Lebedev, *Applications of Tensor Analysis in Continuum Mechanics* (World Scientific, 2018).